SAND89-2403

Discontinuous Behavior Near Excavations in a Bedded Salt Formation*

J. C. Stormont
Repository Isolation Systems Division
Sandia National Laboratories

SAND--89-2403

DE91 004669

Abstract

Discontinuous behavior is being observed and measured in the vicinity of excavations constructed in a bedded salt formation 650 m below ground surface for the Waste Isolation Pilot Plant (WIPP) Facility. The 2 m thick salt layer in the immediate roof acts as a beam, shearing along a thin overlying anhydrite/clay seam. Vertical separations between the immediate roof layer and the overlying strata are often observed at the anhydrite/clay seam above the center of excavations of larger span (11 m). The floor of the excavations is comprised of a 1 m thick salt layer underlain by a 1 m thick predominately anhydrite layer (referred to as MB139). Fractures in MB139 develop beneath most excavations, with increased fracture frequency with drift span and age. In the excavations of larger span (11 m), MB139 eventually debonds along the underlying clay layer. The salt layer overlying MB139 develops both shear and tension failure. In a few locations below excavations of large span, continuous fracture systems are developing from rib to rib through MB139 and the overlying salt. In the ribs, there is limited fracturing within the first meter of most larger excavations. Vertical fractures develop in pillars at most intersections. The discontinuous behavior is qualitatively consistent with analyses of the formation behaving as a layered medium (elastic beam analysis) and limited tensile and compressive failure of the rock salt. The significance of the discontinuous behavior is that it can dominate the effective fluid transport properties of the formation near the excavation, and therefore requires consideration in the design of repository seals. Furthermore, the discontinuous behavior must be monitored and is a very important consideration in the maintenance program designed to assume a safe underground environment.

---

* This paper or article has been accepted for publication in the designated conference proceedings or journal, but many differ from its present form when it is published therein.

Introduction

The Waste Isolation Pilot Plant (WIPP) is a Department of Energy (DOE) facility under development since 1981 near Carlsbad, New Mexico for the purpose of investigating the feasibility of disposing defense-related radioactive waste in a bedded salt formation. Extensive laboratory and field measurements have been directed toward the understanding and modeling of the time-dependent creep behavior of the rock salt. An abundance of field observations and measurements, however, indicate that in addition to the creep behavior there is substantial discontinuous behavior (fractures, separations and shear displacements) in the vicinity of most excavations. A schematic illustration of the observed discontinuous behavior near the largest WIPP excavations is given in Figure 1. These observations are not surprising as discontinuous behavior is routinely observed near excavations in bedded evaporites (e.g., Baar, 1977; Byrne et al., 1979). In the following report some of the discontinuous behavior will be described and discussed, and the conclusion drawn that it is important and/or necessary to consider this behavior when developing a comprehensive model of the behavior of the bedded salt formation.

The WIPP underground facility is located at a depth of 650 m in the Salado formation, a horizontally bedded formation comprised of halite, anhydrite, polyhalite and clay layers. Excavations of numerous dimensions have been created by continuous mining machines at two levels: a simulated-waste experimental level and a storage level. Our discussion will concern only the level at which waste storage is planned.

The first excavations were constructed in 1983 as part of the SPDV (Site Preliminary Design Validation) program, and include an array of four test rooms which are of the same dimensions as the planned waste storage rooms (see Figure 2). Excavation of the actual waste storage rooms began in 1986. The test and storage rooms are 4.6 m high, 11 m wide and 100 m long and are grouped into arrays separated by 33 m pillars; access drifts are in general of smaller width and a similar height. In this discussion, use of the term "room" will refer to the storage room configuration, and "drift" will refer to access excavations which are smaller in span than the storage rooms.

The stratigraphy in the immediate vicinity of the storage level excavations (Figure 3) contains numerous horizontal layers of anhydrite and clay, as well as halite containing various impurities such as clay. The immediate roof above the storage horizon is an approximately 2 m thick layer of relatively pure halite, its upper boundary defined by "Seam B" - a 10 cm thick layer of anhydrite underlain by a thin clay seam. The prominent non-salt bed beneath the storage level excavations is a 1 m thick layer referred to as Marker Bed 139 (MB139). MB139 is quite complex, and comprised of anhydrite, polyanhydrite, halite, and polyhalite, and contains numerous partially infilled subhorizontal fractures. Between MB139 and the floor is a 1 m thick salt layer. The contact with this salt

layer is undulatory with vertical amplitude of .5 m and a wavelength of 1 to 2 m. The lower contact with the salt below consists of a nearly uniform thin clay layer. A detailed characterization of MB139 is given by Borns (1985).

An abundance of instrumentation has been installed in order to monitor the SPDV excavations to identify potential safety concerns, to measure room closure for input to the design of waste handling equipment and operational procedures, and to provide guidance for design modifications and remedial actions (USDOE, 1988). In the access drifts, more than 30 borehole multi-point extensometers and 80 radial convergence points have been installed. At the middle of each test room, stations have been established which include at least 4 extensometers and 4 radial convergence points. Two of the rooms have 30 m deep boreholes in the roof, floor and ribs for inclinometer surveys. Over 150 3 m deep "monitoring boreholes" have been drilled vertically up and down in 30 arrays in the test rooms and along select drifts and intersections for the express purpose of periodic observation and monitoring of discontinuous behavior. Some observations have also been made in more than 100 boreholes which had been previously drilled for various purposes. These boreholes will be referred to as "pre-existing boreholes".

In addition to the geotechnical monitoring at WIPP, there is an extensive program of research-oriented experiments being conducted. The presentation and interpretation of data pertaining to the rock behavior from these experiments are given elsewhere (e.g., Munson et al., 1987).

Behavior of overlying strata

Observations in the 79 vertically-up monitoring boreholes which penetrate Seam B include (USDOE, 1988):

> Shear displacements or offsets often develop along the clay/anhydrite boundary of Seam B. About 1 cm of horizontal shear displacements is typically seen within one year of drilling of the borehole. Such offsetting was found in more than half of all boreholes, and was more than twice as likely to occur near the edge of the excavation compared to the center (USDOE, 1988). Above the majority of excavations, regardless of their size, shear is observed along Seam B near at least one of the ribs.
>
> Vertical separations can occur at Seam B, and are more likely to occur near the center of the excavation than near the edge. The magnitude of the separation is typically limited to less than 3 cm above the test rooms and less than 1 cm elsewhere. These separations are observed to develop within 1 year above the 11 m span test rooms.
>
> There are few observable fractures in the salt layer itself. Some shallow slabbing, at a depth of about 45 cm and most often located near the rib of excavations, has been observed and has

required periodic scaling and/or bolting. A few instances of low angle fractures which extend from near the rib/roof intersection into the salt layer above 11 m span excavations have been observed.

The number of observable fractures and separations increases with time. A survey of the monitoring boreholes in 1986 revealed 17% had discernible fractures; in 1987, the number of boreholes with fractures increased to 33%.

Observations during 1987 in the pre-existing vertically-up boreholes reveal that 41 of the 67 boreholes exhibited separations and/or displacement. Offset or horizontal displacement was observed in 35 of the 67 pre-existing boreholes.

A horizontal displacement is consistently observed on the exposed surface of most rooms and drifts just below the roof/rib contact along a clay parting. The differential displacement moves the rib into the excavation relative to the overlying salt layer.

Extensometers located in vertical boreholes at the center of various size excavations often indicate a differential displacement between anchors on either side of seam B of such a magnitude (more than 5 cm in a few instances above the center of 11 m span excavations) so as to suggest a vertical separation (USDOE, 1988). In two of the test rooms, extensometers located in vertical boreholes near the ribs show that more separation occurs across seam B near one rib compared to the drift center and the other rib.

In these same two test rooms, inclinometer measurements were periodically conducted in vertical boreholes near the rib. Results are given in Figures 4 and 5. Consistent with the borehole observations, shear displacements are seen to occur on the order of 1 cm per year, apparently along or near the Seam B.

Gas flow/permeability measurements made from vertical boreholes over intervals which include Seam B result in very high flows when the test interval is above the center of the excavation, and consistently many orders of magnitude lower when the test interval is near the edge or removed from an excavation (Stormont et al., 1987). The magnitude of the flow, and by inference the size or number of separations, increases as the size of the excavation increases and as the age of the excavation increases. For example, above the center of test rooms more than 2 years old, the permeability of the test intervals which include Seam B was so great that a gas pressure could not be sustained.

Gas flow/permeability measurements in the salt layer itself in the immediate roof indicate a permeability on the order of 10E-6 darcy, considerably greater than the permeability of <1E-9 darcy of "undisturbed" salt more than 5 m away from an excavation. The permeability is not so high so as to suggest mesoscopic fracturing is occurring, but is consistent with permeability measurements made on dilated salt subjected to highly deviatoric, low mean stress

conditions (Peach et al., 1986; Horsemen, 1988). Limited tracer gas measurements indicate the flow paths are larger in the vertical direction than the horizontal direction in the center of the drift.

The measurements and observations are consistent with the immediate roof behaving as a beam which shears in the vicinity of clay/anhydrite Seam B above and the clay parting just below the excavation roof. Such behavior was previously suggested by Stormont et al. (1987) and USDOE (1988). The beam-like shear displacements are occurring to some degree above excavations of all sizes. These displacements reduce shear stresses in the immediate roof, enhancing stability. This is consistent with the observation that at the locations where shear displacement occurs, fewer fractures are observed in the salt layer (USDOE, 1988). In addition to some fracturing, the salt layer in the immediate roof experiences structural changes in the form of dilation. When the combination of the span and age of the excavations is great enough, the immediate roof begins to debond from the remainder of the rock mass, reducing the stability of the excavations.

The inclinometer data given in Figures 4 and 5 reveals additional shear displacement apparently across a clay/anhydrite seam at a depth of 10 to 12 m above the large test rooms. This suggests that the vertical stresses across this layer are relatively small and/or the layer is relatively weak in shear. It is of interest to note that between those layers which shear, there is a clay/anhydrite layer which apparently does not shear. This observation highlights the complex behavior of the rock mass, and suggests the importance of the properties of the discontinuity. Also important is the fact that discontinuous behavior is seen at a depth of 12 m, given that the room has only been open 5 years.

Behavior of underlying strata

Observations in the 87 vertically-down monitoring boreholes which pass through MB139 include (USDOE, 1988):

Beneath the center of excavations of 11 m span, fractures are almost always present in the lower portion of MB139. Vertical separations of 15 cm have been observed beneath the test rooms, but do not exceed 4 cm elsewhere and are usually less than 1 cm.

Shear along the clay layer below MB139 is observed to occur within one year of borehole drilling beneath the center of excavations of 11 m span, and seldom beneath drifts of smaller widths.

The horizontal shear fractures observed in the salt layer above MB139 increase substantially as the size of the excavation increases, and are more often observed near the rib than the center. This salt layer does not appear to debond across the contact with MB139.

The number of observable fractures and separations increases with time. A survey of observation boreholes in 1986 revealed 28% had discernible fractures; in 1987, the number of boreholes with fractures increased to 50%.

Observations during 1987 in the pre-existing vertically-down boreholes reveal that 31 of the 44 boreholes exhibited separations and/or displacement. Offset or horizontal displacement was observed in 21 of the 44 pre-existing boreholes.

A few fractures are exposed on the floor surface. Detailed mapping of such fractures reveals that in some 11 m span excavations, an arcuate or dish-like fracture system concave toward the opening is developing (Borns and Stormont, 1988; USDOE, 1988).

Extensometer measurements made from vertical boreholes near the center of 11 m span rooms and the intersections of these rooms and access drifts almost always reveal some vertical separation developing within MB139 (USDOE, 1988).

Inclinometer measurements conducted in vertically-down boreholes near the ribs of two 11 m span rooms indicate shear offsets along the bottom of MB139 (USDOE, 1988). Refer to Figures 6 and 7. The shear displacements are on the order of about 1 cm/year.

Gas flow/permeability measurements made over test intervals which include MB139 indicate (Stormont et al., 1987; Borns and Stormont, 1988):

Flow rates in MB139 near the center of excavations of comparable age increase as the span of the drift increases (Figure 8). In 4 of 7 tests conducted from the center of test rooms (11 m span) in which the test intervals included MB139, the permeability was so great a gas pressure could not be sustained.

Flow rates increase as the age of the opening increases; however, the influence of span appears to be more important (Table 1).

Low flow rates are measured in test intervals located near the edge of excavations.

Gas flow/permeability measurements made beneath the center of 6.6 m span drifts indicate permeabilities in the salt layer above MB139 of about 1E-5 darcy, which is appreciably greater than the permeability of intact or undisturbed salt. Tracer gas measurements made in various size drifts have shown that the 1 m thick layer of salt has larger vertical than horizontal flow paths (equivalent apertures), and that the dimension of these flow paths increase an order of magnitude from about 2E-5 m to 2E-4 m as the drift span increases from 6.6 m to 11 m (Borns and Stormont, 1988).

The observations and measurements taken together suggest that the immediate floor exhibits three progressive, discontinuous behaviors:

1. Horizontal fracturing develops in the lower parts of MB139, most often near the center of drifts of all sizes. The degree and frequency of fracturing increases with the drift span and time.

2. Shear displacement occurs along the contact between the MB139 and the underlying strata. The salt layer above MB139 appears to remain bonded to MB139 but develops horizontal shear fractures. This behavior is almost always seen beneath drifts of larger span which have been open for more than about 3 years.

3. High angle fractures develop in both MB139 and the overlying salt layer near the rib. This failure is not along pre-existing weakness planes, and essentially debonds the immediate MB139 from the remainder of the rock mass.

Behavior of ribs

Most ribs at the storage horizon exhibit shear displacement of the rib along a clay parting near the intersection with the roof, as mentioned in the discussion of the roof behavior and illustrated in Figure 1.

Within the first meter of most excavations, some fractures parallel to the drift are observed from boreholes at the midheight of the rib (USDOE, 1988; Borns and Stormont, 1988). In this region, the permeabilities are generally greater (about 1E-4 darcy) than at any other location in the salt. Between 1 and 2 meters into the rib, permeabilities decrease to the 1E-6 darcy level and below, and beyond 2 meters the permeabilities rapidly decrease to the value associated with intact salt (<1E-9 darcy).

Vertical fractures, up to 10 cm wide, form at the corners of most intersections within 3 months of excavation (USDOE, 1988). Most corners require periodic scaling, as well as rock bolts and wire mesh.

Analyses

The response of rock surrounding excavations in bedded salt is very complicated, involving salt creep, movement along planes of weakness or discontinuities, strain softening, and development of fractures. Further, the rock response may involve coupled hydrologic-mechanical processes given the brine and gas known to exist in the formation. A comprehensive model of rock behavior taking all of the above factors into account is not available. Previous numerical analyses of the rock response have focused on the creep behavior of the salt; failure has not been included in these analyses, nor has coupled hydrologic-mechanical behavior. However, some indication that discontinuous behavior is expected can be gathered by means of various conventional analyses or examination of previous results.

1. Rock behavior as a layered medium - Consideration of the immediate roof and floor of the test rooms as a layered medium is consistent with the observed discontinuous behavior surrounding WIPP excavations. Elastic beam analysis, albeit simplistic, provides some insight into the behavior of the roof and floor layers. Beam formula for various loading and boundary conditions are summarized by Wright (1973).

The salt layer from the roof to the clay/anhydrite seam 2 m above the excavations (Seam B) can be considered as a distinct layer or beam. The boundary condition at the abutment was estimated to lie between a fixed and simply supported beam by considering the rigidity of the pillars with respect to the beam (Wright, 1973, Eqn. 11 and 12). For an elastic beam subjected to a horizontal load and a load from the overlying strata with this boundary condition, the maximum bending stresses occur at the center of the beam and the maximum shear stresses occur at the abutment. In the absence of horizontal loading, the weight of the beam itself would induce horizontal tensile stresses at the center of the beam (about 1 MPa) approaching the tensile strength of the salt itself (<2 MPa); any loading from the overlying salt above the beam would induce even greater tensile stresses. Mesoscopic vertical tensile fractures associated with horizontal tensile stresses are not observed, strongly suggesting there are substantial horizontal loads on the roof beam. Assuming a frictionless contact with the overlying strata, the horizontal or axial stress (σ) in the beam is a maximum at the top and bottom of the beam and is given by

$$\sigma = p \pm 6M/d^2 \qquad (1)$$

where p is the axial load per unit width per unit depth, d is the beam depth, and M is the moment per unit width. The maximum moment for these boundary conditions is at the beam midspan and is approximately

$$M = qL^2/12 \qquad (2)$$

where q is the distributed vertical load per unit width per unit depth and L is the beam length. Combining (1) and (2) yields a relationship for the axial stress on the top and bottom of the beam at midspan as a function of the axial and overlying loads

$$\sigma = p \pm qL^2/(2d^2) \qquad (3)$$

In Figure 9, we plot the combination of vertical and overlying distributed load which result in the axial stress exceeding the tensile strength at the bottom of the beam. These results imply the salt layer comprising the immediate roof is subjected to substantial horizontal loads and relatively low vertical loads. The observed trend is that in bigger and older excavations, the beam is progressively debonding; that is, the salt layer comprising the immediate roof is deforming (creeping) faster from the combination of axial horizontal load and its own weight than the overlying main roof is.

For the underlying strata, the salt layer immediately below the excavation and MB139 can also be thought of as separate and distinct layers or beams. As with the roof beam, the boundary condition at the abutment lies between a fixed and simply supported beam. Therefore, the maximum horizontal compressive stresses will occur at the bottom of MB139 below the excavation center according to Equation (3). The high compressive stresses could result in failure along the numerous pre-existing planes of weakness within the MB139 layer. This result is consistent with the observed fractures in the lower portion of MB139 underneath the center of excavations along pre-existing planes of weakness, and that the size and number of these fractures increases with the excavation span. High horizontal stresses would enhance such failure, and would tend to suppress vertical tensile fractures in the overlying salt. Eventually, with an increasing distributed load (from creep of the underlying salt), tensile fractures in the overlying salt will develop. Finally, given a sufficient combination of drift span and distributed load, the salt and anhydrite near the abutment will fail either due to horizontal shear failure or high angle tensile failure. The maximum horizontal shear stresses (τ) are at the middle of the beam

$$\tau = 3V/(2d) \tag{4}$$

where V, the shear force per unit width, is a maximum at the abutment and is approximately

$$V = qL/2 \tag{5}$$

Combining (4) and (5) yields

$$\tau = 3/4\ (qL/d) \tag{6}$$

The horizontal shear stresses are unaffected by the axial load. The maximum tensile stress at the abutment due to the overlying load is equal to the magnitude of the shear stress and occurs at 45° to the horizontal, and is modified by the axial load as follows

$$\sigma = 1/2\ p - 3/4\ (qL/d) \tag{7}$$

We compare the criteria for horizontal shear failure (Equation 6) with that for the high angle extensional failure (Equation 7) at the abutment in Figure 10 assuming a shear and tensile strength for the anhydrite of 43 and 6 MPa, respectively. We find the combination of horizontal and distributed vertical load required for high angle extensional failure at the abutment in the anhydrite is much less than that for horizontal shear failure. The observed high angle fractures in the anhydrite and salt beneath the abutment of the largest excavations are qualitatively consistent with this result.

The above analysis assumed the clay seams provide a frictionless contact between layers. A more realistic representation of the clay seams is a Mohr-Coulomb material, where in the absence of cohesion the shear strength (τ) along a surface is proportional to the normal stress (σ)

$$\tau = \mu\ \sigma \tag{8}$$

The coefficient of friction, μ, has a great influence on the behavior of the rock near excavations. Stone et al. (1981) conducted a numerical study of the effect of clay seams on the response of WIPP excavations. As illustrated in Figure 11, as μ was increased from 0.0 to 1.0, closure decreased by a factor of three. The closure can also be seen to be most sensitive to values of μ below 0.5. In a separate study of the response of WIPP excavations, Munson et al. (1989) found that decreasing μ from the reference value of 0.4 to 0.2 resulted in an increase in the calculated closure for drifts constructed at the simulated-waste experimental level. This reduced value of μ was considered to be more consistent with the observed in situ behavior of clay seams, and helped reconcile calculated and measured closure (Munson et al., 1989).

Such analyses, coupled with the observations and measurements, suggest the clay seam properties and behavior are key factors in the stability and behavior of the rock surrounding WIPP excavations.

2. Failure due to tensile stresses - Morgan (1985) reviewed numerous previous finite element calculations to determine if they indicated a potential for failure in the rock surrounding WIPP excavations. These calculations incorporated the major features of the bedded salt stratigraphy surrounding WIPP excavations (salt, anhydrite and clay), and limited slip along clay seams was allowed. Although these calculations focused on the time-dependent deformation of the salt, and did not explicitly account for failure, the potential for failure or cracking could be identified by the existence of tensile stresses. Since failure was not modeled in the calculations, progressive failure could not be assessed.

For models of the storage room configuration, small areas of vertical tensile stresses were found to develop instantaneously after excavation in the salt near the surface of the room in both the floor and the roof. The zone of vertical tensile stresses grew modestly for about one-half year, but then stopped. Horizontal tensile stresses develop shortly after excavation in salt in the middle of pillars between rooms and in the floor of the rooms, as well as in MB139 near the center of the pillar. The regions of horizontal tensile stress were found to increase with time, particularly in the anhydrite. Morgan concluded that the previous calculations suggest tensile stresses originate in the salt and then move toward the anhydrite layers, and the regions of tensile stress change little one-half year after excavation.

3. Failure of rock salt under compressive stresses - Failure of rock can also occur under compressive stress conditions. From a series of quasi-steady triaxial compression and indirect tension tests for various rock salts, Pfeifle et al. (1983) derived a failure criterion of the form

$$F = J_{2D}^{1/2} - K - a(1 - e^{-J_1}) \qquad (9)$$

where J_{2D} is the second invariant of the deviatoric stress tensor, J_1 is the first invariant of the stress tensor, and a, b, and k are

empirical constants. A positive value of F incidates failure. Failure was assumed when either a peak stress was achieved or when a large axial strain limit (15%) was exceeded. For bedded salt from the Permian basin in Texas, the empirical constants were determined to be

$k = 1.0$ MPa
$a = 38.8$ MPa
$b = 0.0174$ MPa^{-1}

Finite element calculations of stress and strain fields surrounding WIPP excavations by DeVries (1988) were used to evaluate the above failure criterion. These calculations assumed the stratigraphy was comprised solely of salt. The model parameters for the time-dependent deformation of the salt were adjusted until predicted and measured deformations surrounding WIPP excavations matched reasonably well. Contours of the value of F computed from these calculations surrounding a 5.4 m high by 5.4 m wide drift immediately after excavation are given in Figure 12. Regions of stress states which exceed the failure criterion are identified by positive F values. Immediately after excavation, there is a region of failure in the middle of the ribs and the roof and floor adjacent to the drift. In Figure 13, the F=0 contours at 0, 1 and 5 years after excavation are given, and reveal that the stress conditions which satisfy or exceed the failure criterion decrease somewhat with time.

An alternative approach for assessing the potential for failure under compressive stresses is to consider a crack initiation criterion. In the Griffith theory, failure occurs when the most vulnerably oriented crack in a population of randomly oriented cracks begins to extend under applied stress. The boundaries between rock salt crystals may be considered as a random system of closed cracks. When the friction of closed cracks is taken into account, the Griffith criterion becomes (Paterson, 1978)

$$M = (\sigma_1/4)[(\tan^2\phi+1)^{1/2}-\tan\phi] - (\sigma_3/4)[(\tan^2\phi+1)^{1/2} + \tan\phi] \quad (10)$$

where $\tan\phi$ is the coefficient of friction between crack surfaces. When M is a positive value, the potential for crack extension or opening will exist due to the presence of tensile stresses on the crack surfaces.

Application of the Griffith criterion to macroscopic or final failure has been less than satisfactory because the theory deals with initiation of failure on the scale of cracks, which typically occurs considerably below the macroscopic failure stress (Paterson, 1978). However, such a criterion may be particularly suited for identification of the potential for dilatant behavior. Dilatancy is defined as net volume increase under compressive stresses due to the formation and extension of open microcracks (Jaeger and Cook, 1979). Because dilation introduces void volume to the material, it can be considered (at least in part) as discontinuous behavior.

Contours of the value of M computed from the finite element calculations of DeVries surrounding a 5.4 m high by 5.4 m wide drift

immediately after excavation are given in Figure 14. Regions of positive M values are seen to develop immediately after excavation. The extent of this region doesn't appreciably change with time, as illustrated in Figure 15 by the M=0 contours at 0, 1 and 5 years after excavation. The internal friction angle used in calculating the Griffith contours was the value reported for two surfaces of rock salt in contact (μ = 0.70) by Bowden and Tabor (1964). Reported values for the internal friction coefficient derived from quasi-static tests on bedded salt samples vary from 0.73 (Fuenkajorn and Daemen, 1988) to 1.73 (Hansen et al., 1983). Larger values of μ reduce the size of the zone where tensile stresses exist on crack surfaces.

Because dilatancy in rock salt does not necessarily imply a loss of strength or softening (e.g., Wawersik and Hannum, 1980; Fuenkajorn and Daemen, 1988), it would be expected to be initiated at stresses which are lower than those required for macroscopic failure. The results given in Figures 12 and 14 are consistent with this observation. A dilatant zone of rock salt was previously proposed to explain the distribution of gas permeabilities measured in the rock salt surrounding WIPP excavations (Stormont et al., 1987). As illustrated in Figure 16, the regions of increased gas flow rates (and consequently gas permeabilities) are qualitatively consistent with the crack initiation or dilation criterion contours in Figure 14.

The above analysis indicates the potential for limited failure or structural change of the rock salt surrounding WIPP excavations. Because the calculations indicate the stress conditions for such failure do not worsen with time, the behavior should manifest itself concurrent with or shortly after excavation. However, as with Morgan's analysis of tensile failure, the failure process itself is not included in the calculations so estimates of time-dependent failure are speculative.

Discussion

The field observations reveal that discontinuous behavior in the form of fractures, separations and shear displacement are common in the vicinity of WIPP excavations, and that the frequency of these observations increases with the excavation span and age. This conclusion is summarized in Figure 17, where the relationship between the number of borehole arrays which had some discernible fractures as a function of drift span and time is given. Because the vast majority of waste storage will occur in the largest excavations, it follows that appreciable discontinuous behavior should be expected in waste storage areas. It is important to recognize that the discontinuous behavior described herein has been observed in excavations which are less than 5 years old. The frequency and extent of such behavior will increase with time, and as the planned life of the WIPP facility is 20 to 30 years, may impact operational and post-closure (sealing) activities.

The mission of the WIPP Facility has significant requirements for excavation stability. During the experimental phase, access must be maintained to the storage rooms because of the possibility of retrieval of the waste within in the first 5 years after disposal. The potential for serious instability will have to be closely monitored, and aggressive remedial action taken where necessary. The number of roof bolts installed in 1987 was four times the number installed in all previous years, portending the magnitude of the maintenance effort. It is reasonable to expect that stable openings can be maintained in the salt with appropriate maintenance efforts since numerous potash and salt mines have been operated safely for several decades using accessways that are routinely maintained.

Discontinuous behavior may have an impact on the effectiveness of the long-term isolation of waste. Upon filling the repository with waste, the repository will be sealed with a series of man-made structures in order to limit the flow in, through and out of the repository. The effectiveness of the seal system depends not only on the seal itself, but also on the permeability of the adjacent rock. While intact or undisturbed rock has a very low permeability, the presence of discontinuities can dramatically increase the bulk fluid transport properties of the rock. For example, the presence of 0.1 mm wide fractures spaced 1 m apart changes the effective permeability of rock salt from 1E-9 darcy to 1E-4 darcy. Furthermore, the discontinuities tend to develop along the axes of excavations and therefore require consideration when designing the seal systems. Even in the case when discrete or observable discontinuities or fractures do not develop, rock salt may dilate. In the case of dilated rock salt, the flow paths can be very small (on the order of 10E-6 m) but still result in a 3 orders of magnitude increase in permeability with respect to that of undisturbed rock salt.

Certainly the development of fractures, separations and shear displacements will alter stress, strain and displacement fields. When the discontinuous behavior reduces the material's load-carrying capability (strain softening), stress differences will be pushed farther out into the rock mass. Because salt creep is driven by deviatoric stresses, more closure would be expected. In the extreme case of complete debonding of a layer such as observed in the strata underlying a few of the largest and oldest WIPP excavations, the effective boundary of the excavation is extended. For steady-state creep, the closure of an excavation scales proportionally to its effective opening size; therefore, increasing the size of an opening will result in more closure. Even discontinuous behavior which does not result in softening (such as dilation of salt under some conditions) will affect the properties of the rock mass and its subsequent behavior. For example, if a zone of rock salt surrounding WIPP excavations develops a crack system and dilates, the elastic moduli will be reduced as the crack density increases (e.g., Budiansky and O'Connell, 1976).

In summary, we conclude that there is an abundance of observations of discontinuous behavior surrounding WIPP excavations, consistent with mining industry experience and conventional analyses. With

increasing age of the excavations, the discontinuous behavior will require an ever-increasing effort in order to maintain access and stability. Further, we recognize that the observed discontinuous behavior is a component of the overall rock mass behavior, and should be considered in formulating or interpreting predictive models for the long-term mechanical response of bedded rock salt to excavation. Finally, the discontinuous behavior may dominate the near-field fluid transport properties of the formation and must be considered in seal systems designed to isolate waste.

References

C. A. Baar, Applied Salt-Rock Mechanics 1, The In Situ Behavior of Salt Rocks, Elsevier Scientific Publishing Co. Ltd., 1977.

R. J. Byrne, C. M. Koplik, S. G. Oston, M. S. Giuffre, L. R. Meyer, and D. L. Pentz, Mine Structural Features, Volume 4 of Information Base of Waste Repository Design, US Nuclear Regulatory Report NUREG/CR-0495, March 1979.

D. J. Borns, Marker Bed 139: A Study of Drillcore from a Systematic Array, Sandia National Laboratories Report SAND85-0023, 1985.

D. J. Borns and J. C. Stormont, An Interim Report on Excavation Effect Studies at the Waste Isolation Pilot Plant: Delineation of the Disturbed Rock Zone, Sandia National Laboratories Report SAND87-1375, 1988.

F. P. Bowden and D. Tabor, The Friction and Lubrication of Solids, Vol. 1, Clarendon Press, 1964.

B. Budiansky and R. J. O'Connell, Elastic Moduli of a Cracked Solid, International Journal of Solids and Structures, Vol.12, p. 81-97, 1976.

K. L. DeVries, Structural Calculations for Permeability Test Interpretation, Technical Letter Memorandum RSI/TLM-156 to J. G. Arguello, ReSpec, Inc., October 18, 1988.

K. Fuenkajorn and J. J. K. Daemen, Borehole Closure in Salt, US Nuclear Regulatory Commission Report NUREG/CR-5243, December, 1988.

F. D. Hansen, K. D. Mellegard and P. E. Senseny, Elasticity and Strength of Ten Natural Rock Salts, Mechanical Behavior of Salt I, Proceedings of the First Conference on the Mechanical Behavior of Salt, The Pennsylvania State University, p. 71-84, 1981.

S. T. Horsemen, Moisture Content - A Major Uncertainty in Storage Cavity Closure Prediction, Second Conference on the Mechanical Behavior of Salt, Trans Tech Publications, p. 55-68, 1988.

J. C. Jaeger and N. G. W. Cook, Fundamentals of Rock Mechanics, Third Edition, Chapman and Hall, 1979.

H. S. Morgan, C. M. Stone, and R. D. Krieg, An Evaluation of WIPP Structural Modeling Capabilities Based on Comparisons with South Drift Data, Sandia National Laboratories Report SAND85-0323, 1986.

D. E. Munson, A. F. Fossum, and P. E. Senseny, Approach to First Principles Model Prediction of Measured WIPP In Situ Room Closure in Salt, 30th US Symposium on Rock Mechanics, University of West Virginia, June 19-22, 1989.

D. E. Munson, R. L. Jones, D. L. Hoag, and J. R. Ball, Heated Axisymmetric Pillar Test (Room H): In Situ Data Report (February 1985- April 1987) Waste Isolation Pilot Plant Thermal/Structural Interactions Program, Sandia National Laboratories Report SAND87-2488, October, 1987.

M. S. Paterson, Experimental Rock Deformation - The Brittle Field, Springer-Verlag, 1978.

C. J. Peach, C. J. Spiers, A. J. Tankink, and H. J. Zwart, Fluid and Ionic Transport Properties of Deformed Salt Rock, Commission of the European Communities Report EUR 10926, 1987.

T. W. Pfeifle, K. D. Mellegard, and P. E. Senseny, Constitutive Properties of Salt from Four Sites, Office of Nuclear Waste Isolation Report ONWI-314, April, 1983.

C. M. Stone, R. D. Krieg and L. J. Bransetter, The Effects of Clay Seam Behavior on WIPP Repository Design, Sandia National Laboratories Report SAND81-0768, 1981.

J. C. Stormont, E. W. Peterson, and P. L. Lagus, Summary of and Observations About WIPP Facility Horizon Flow Measurements Through 1986, Sandia National Laboratories SAND87-0176, 1987.

USDOE, Geotechnical Field Data and Analysis Report, July 1986 through June 1987, DOE/WIPP Report 87-017, 1988.

W. R. Wawersik and D. W. Hannum, Mechanical Behavior of New Mexico Rock Salt in Triaxial Compression Up to 200oC, Journal of Geophysical Research, Vol. 85, p. 891-900, 1980.

F. D. Wright, Roof Control through Beam Action and Arching, SME Mining Engineers Handbook, American Institute of Mining, Metallurgical and Petroleum Engineers, Vol 1, p. 13-80 - 13-86, 1973.

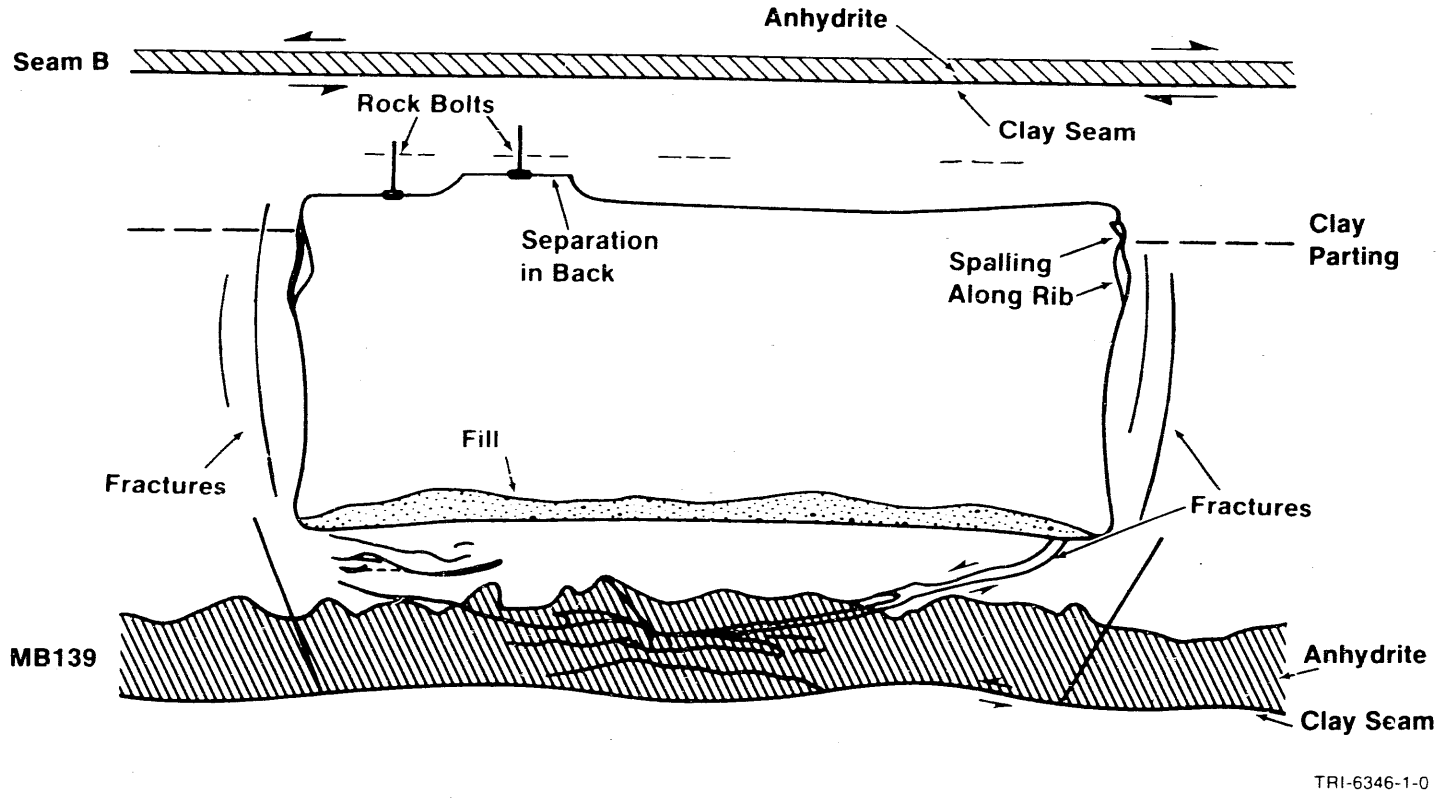

Figure 1. Observed discontinuous behavior near 4 m by 11 m test rooms (from Borns and Stormont, 1988).

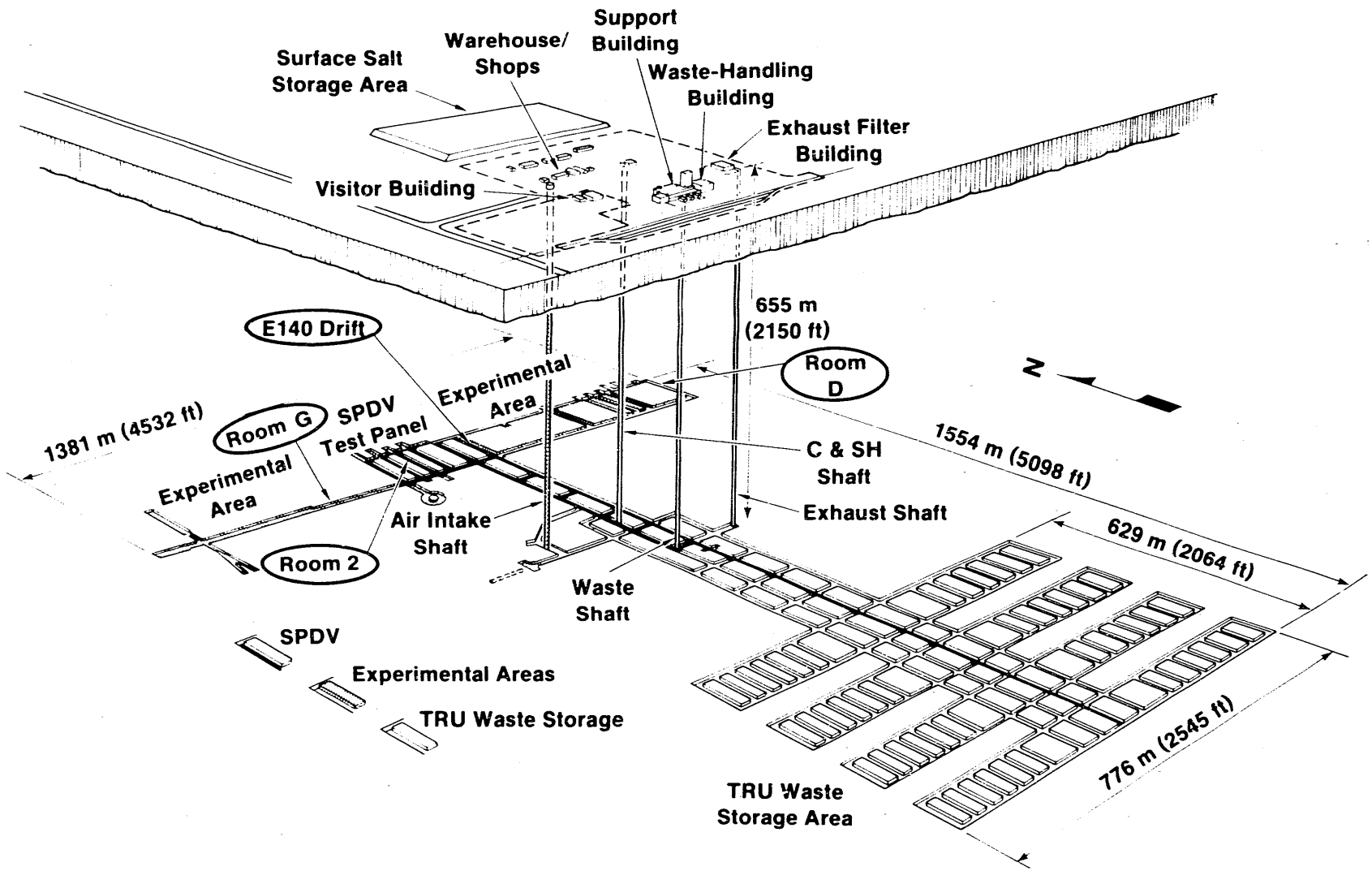

TRI-6346-16-0

Figure 2. The WIPP Facility.

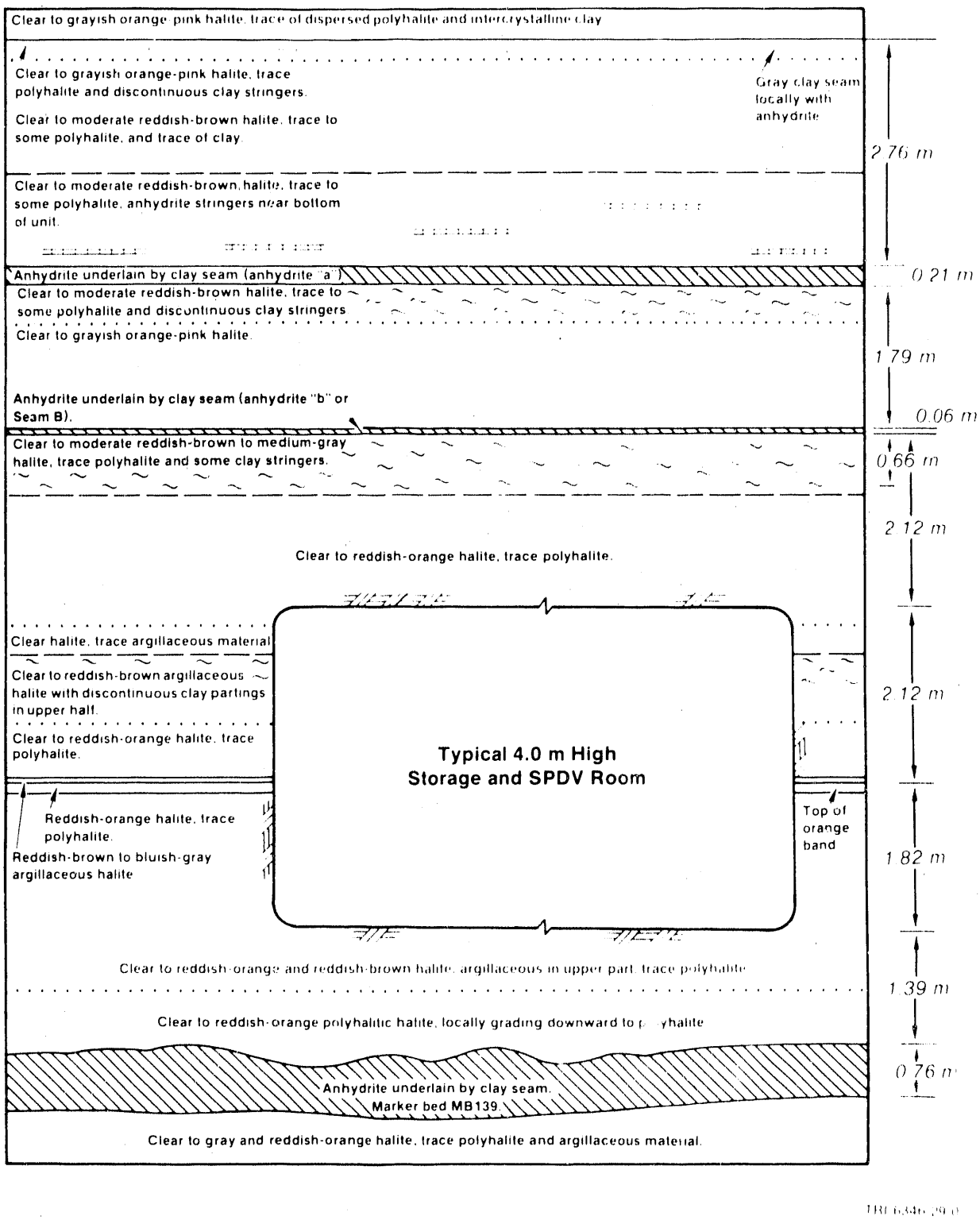

Figure 3. Stratigraphy in the vicinity of WIPP excavations.

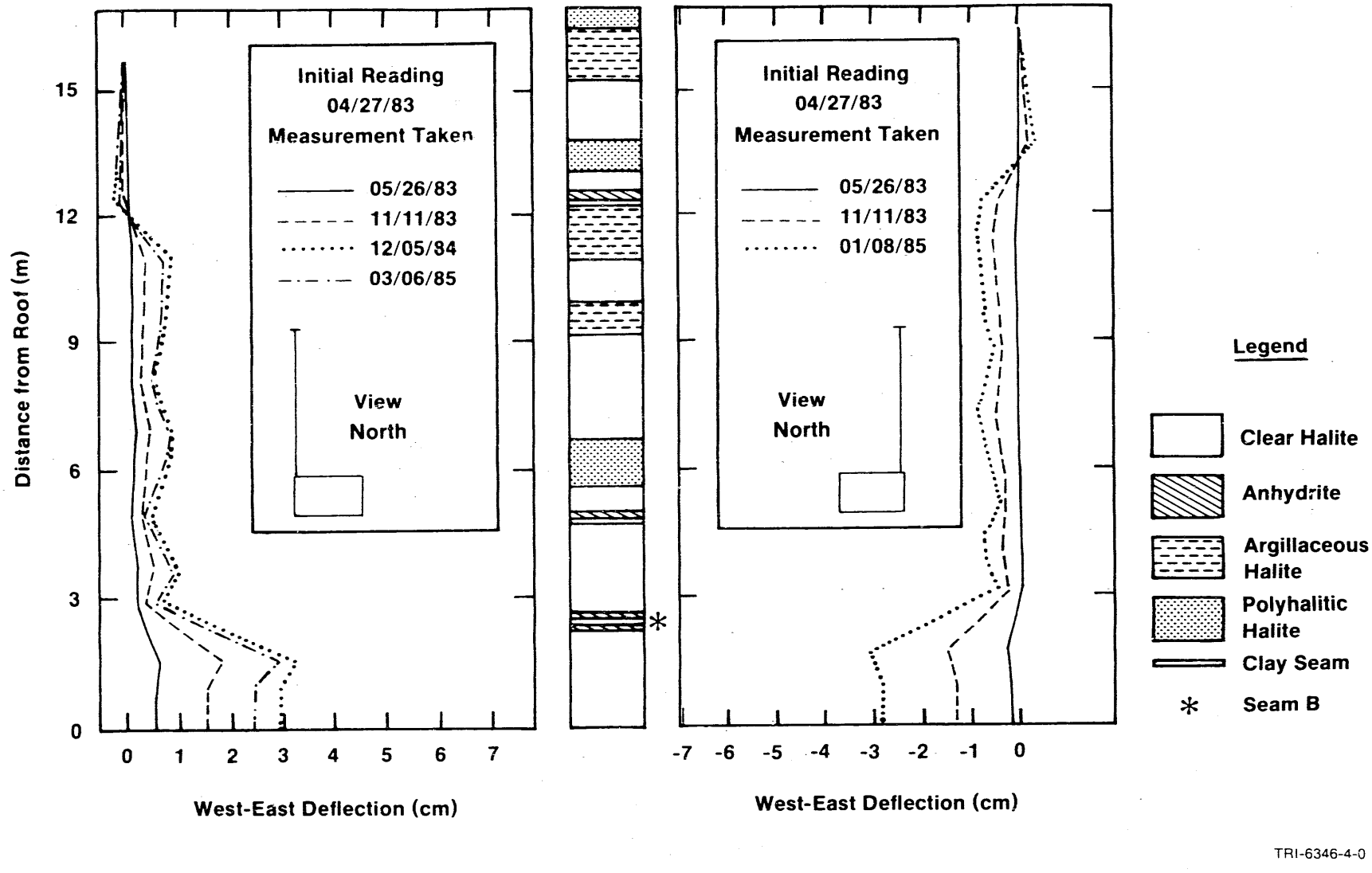

Figure 4. Results from vertically-up inclinometer surveys in test room 1 (from USDOE, 1988).

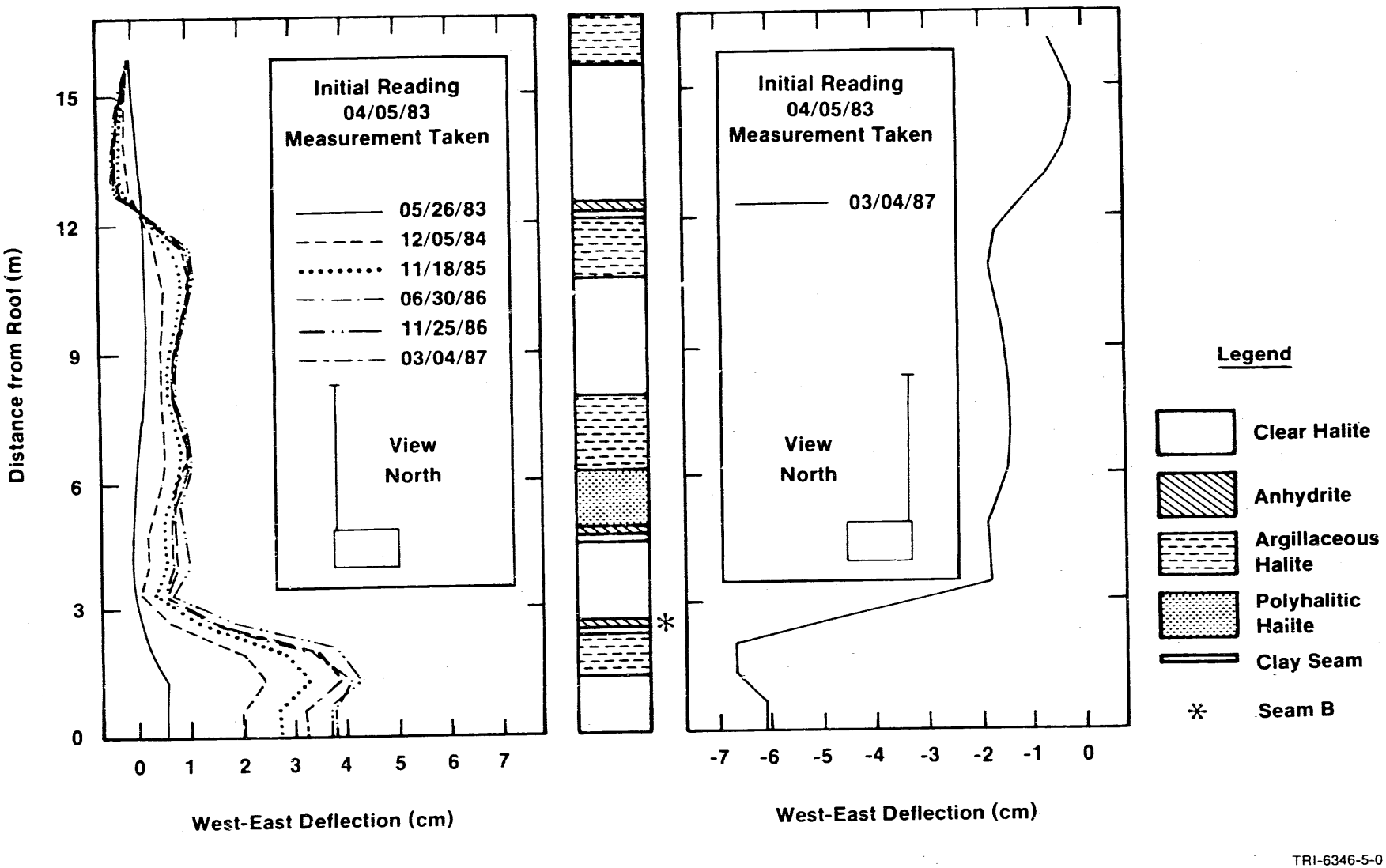

Figure 5. Results from vertically-up inclinometer surveys in test room 2 (from USDOE, 1988).

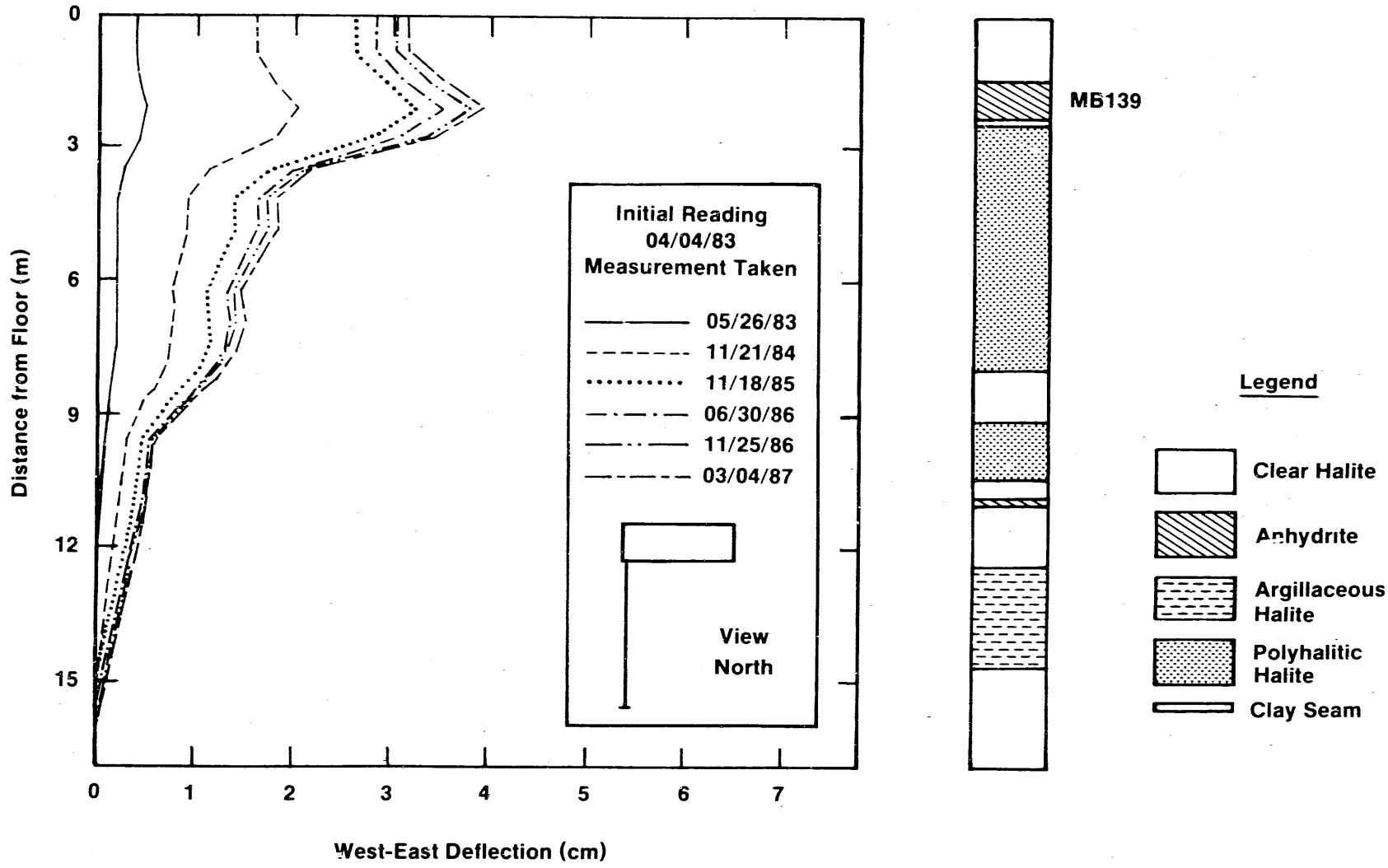

Figure 6. Results from vertically-down inclinometer surveys in test room 1 (from USDOE, 1988).

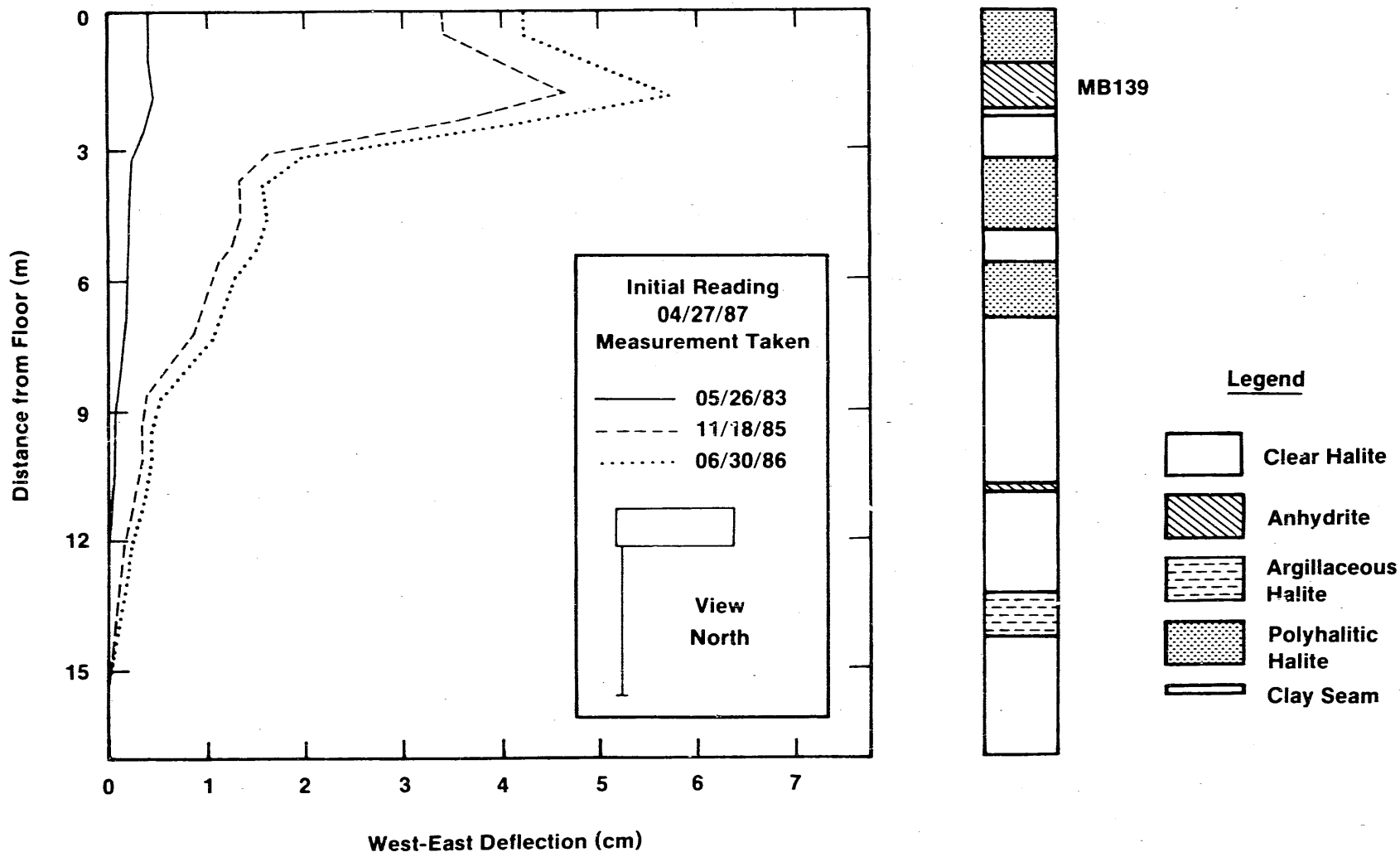

Figure 7. Results from vertically-down inclinometer surveys in test room 2 (from USDOE, 1988).

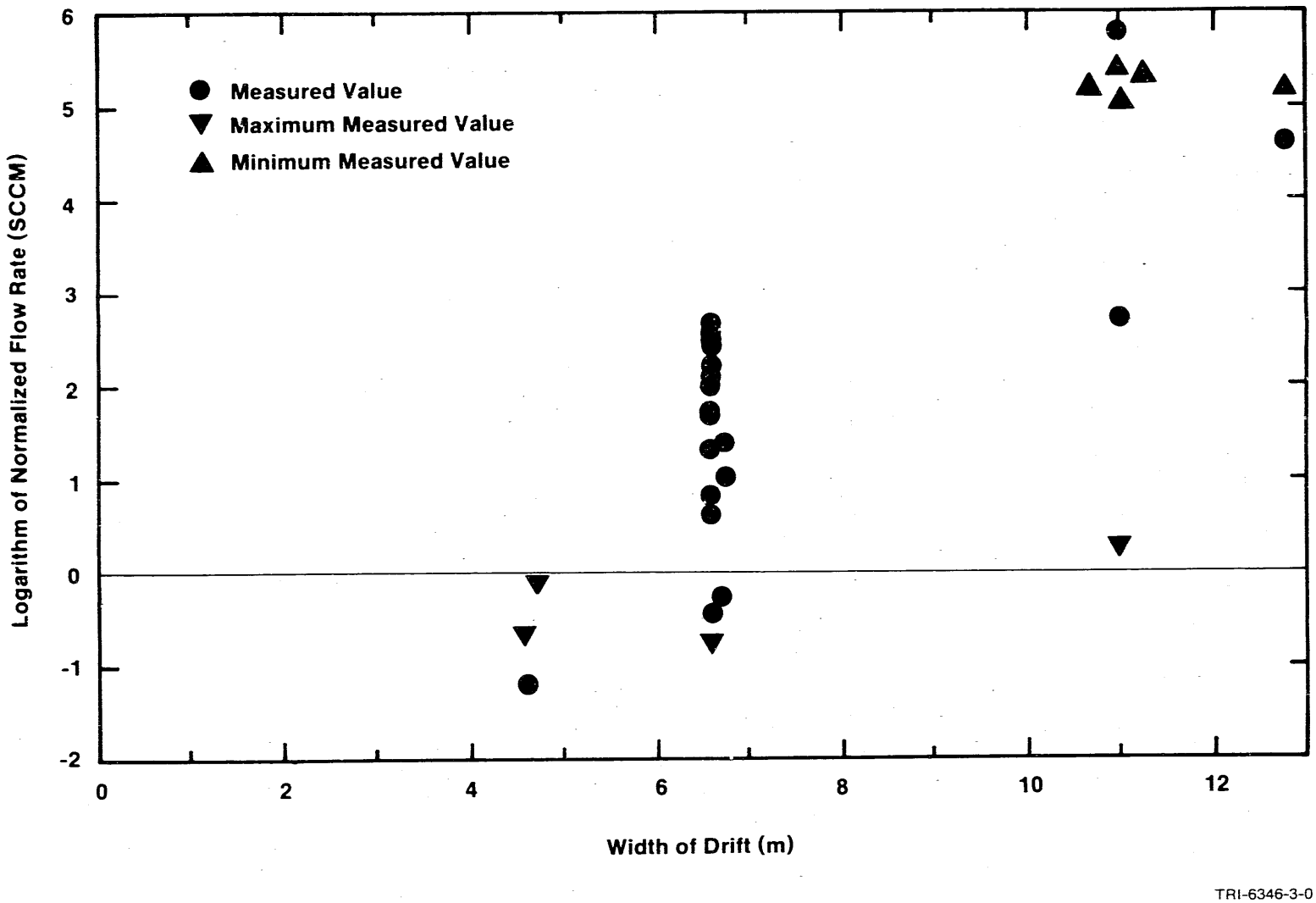

Figure 8. Injected gas flow rate vs. drift width for test intervals including MB139 (from Stromont et al., 1987).

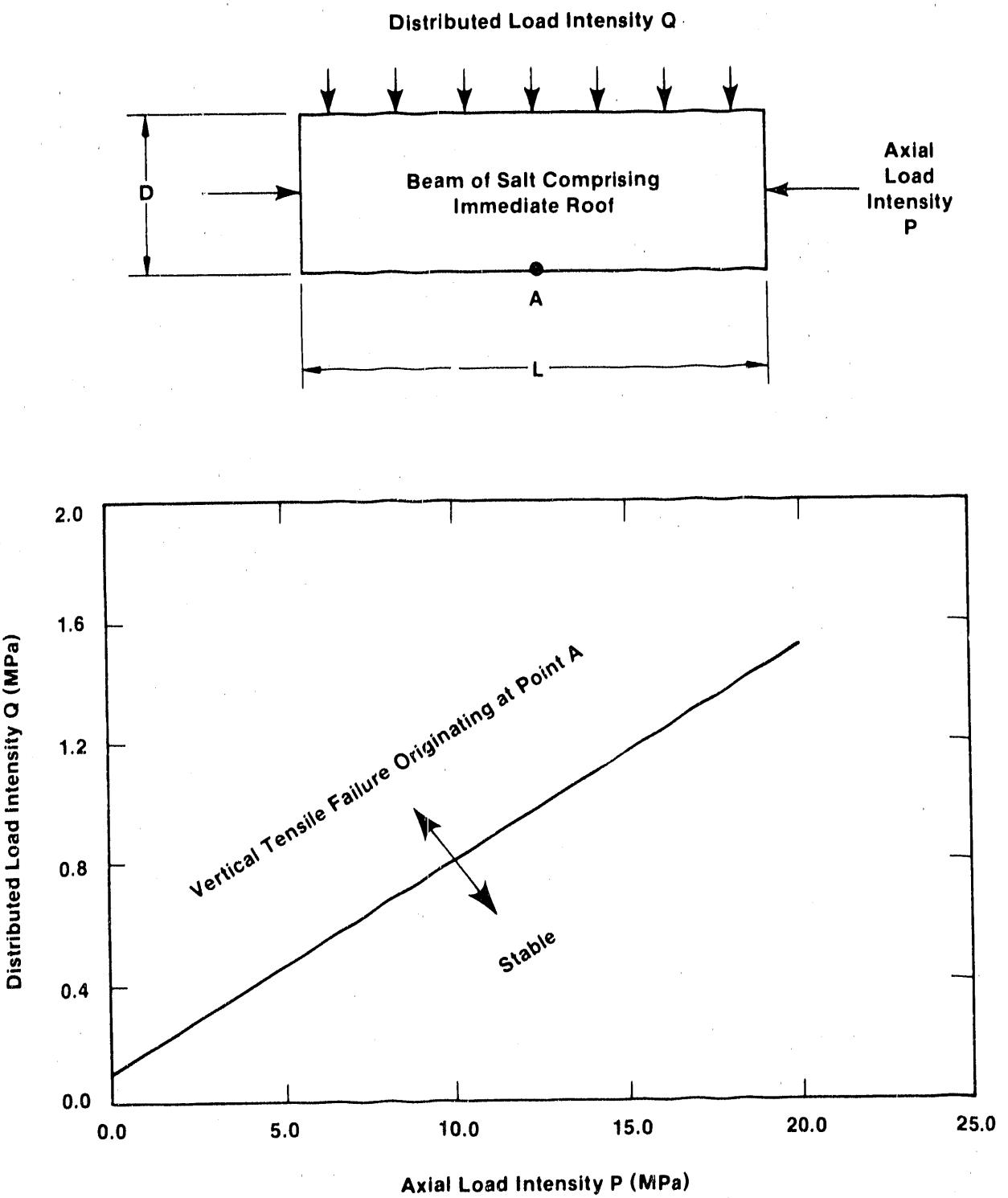

Figure 9. Results from elastic beam stability analysis of salt layer in immediate roof. The stability criterion is given as a function of the distributed overlying load intensity and axial horizontal load intensity.

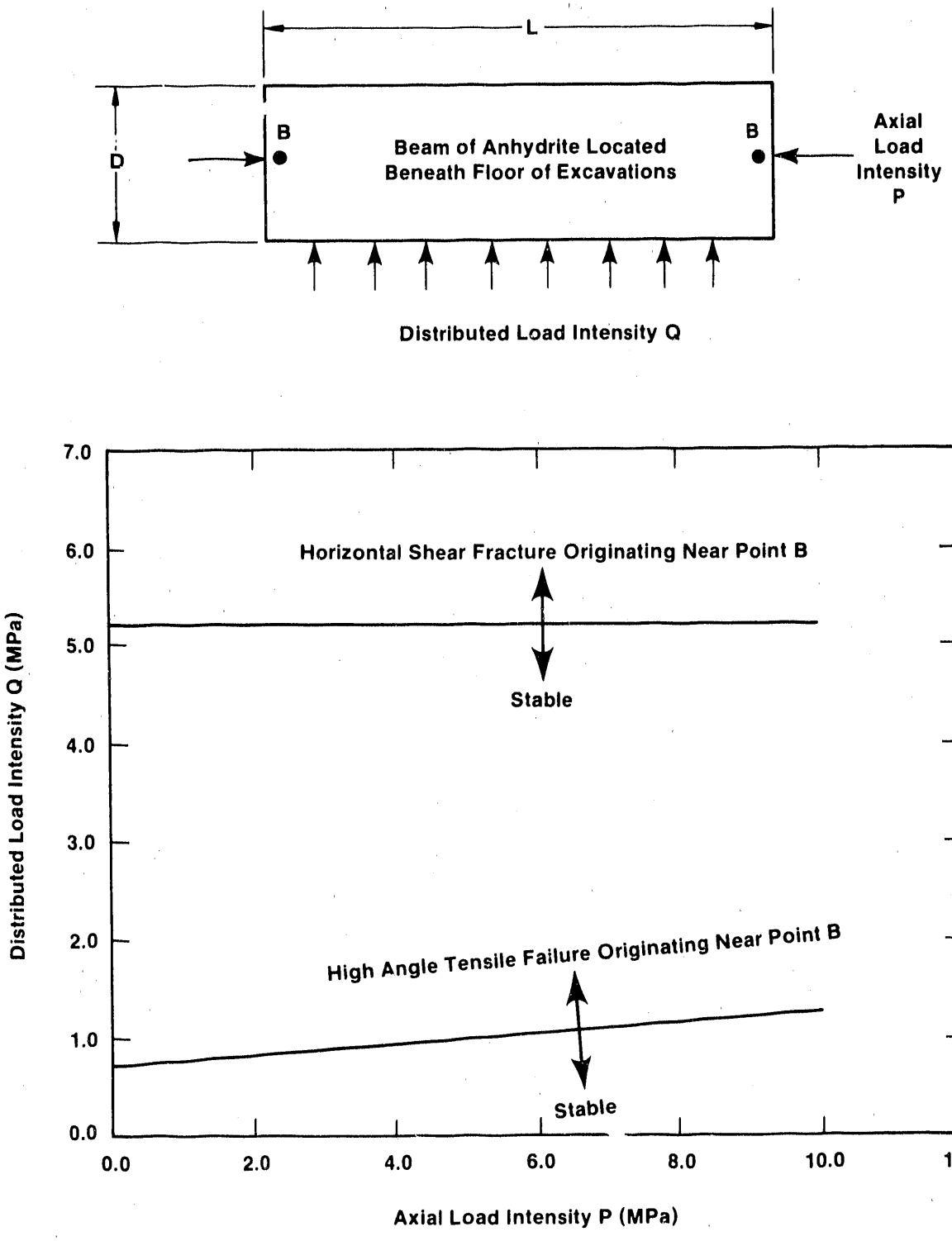

Figure 10. Results from elastic beam stability analysis of MB139. The stability criterion for both high-angle extensional failure and horizontal shear failure are given as functions of the distributed load intensity on the underside of the beam and the axial horizontal load intensity.

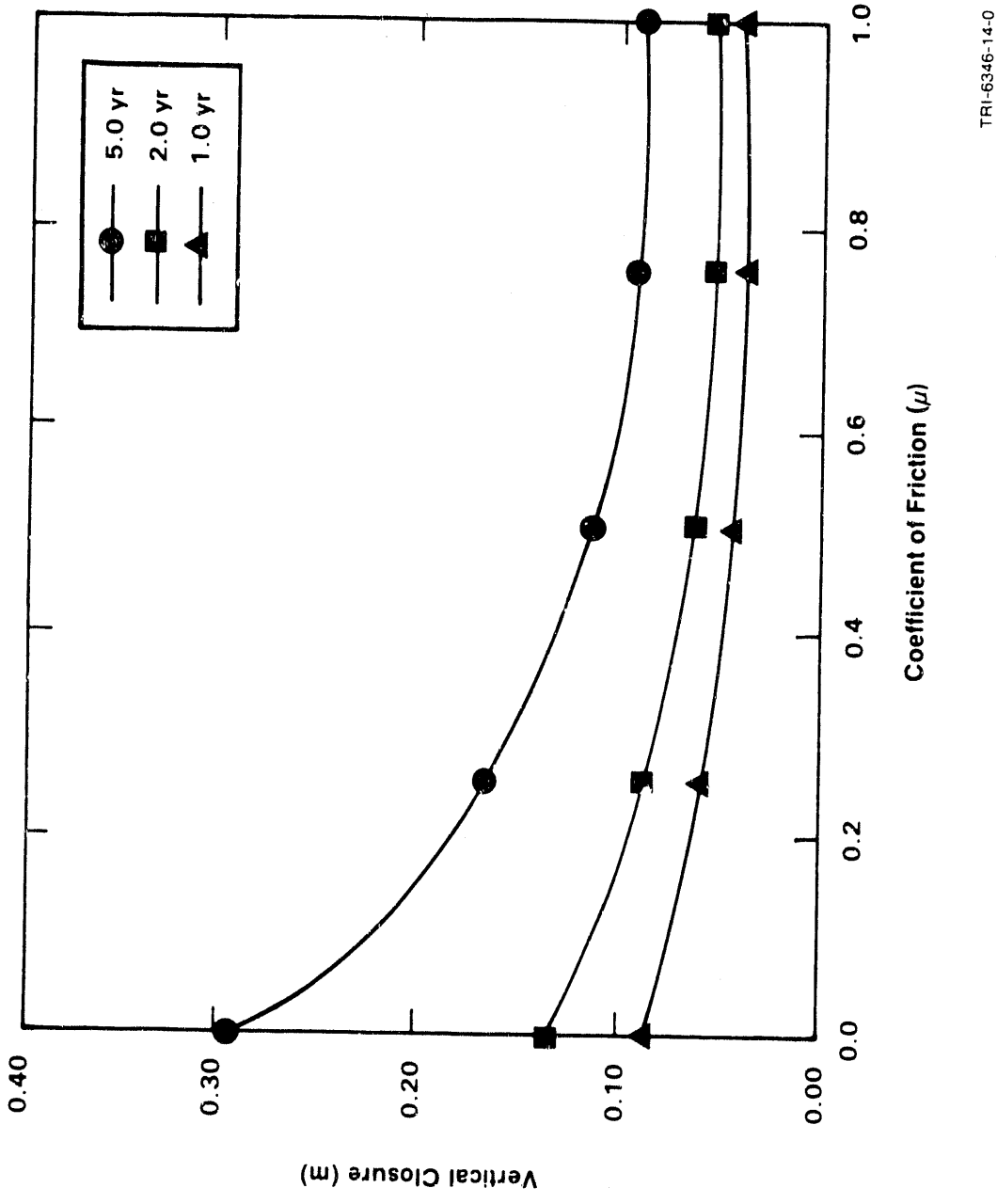

Figure 11. Calculated vertical closure for 4 m by 5 m drift at 1, 2 and 5 years after excavation as a function of the clay seam coefficient of friction (from Stone et al., 1979).

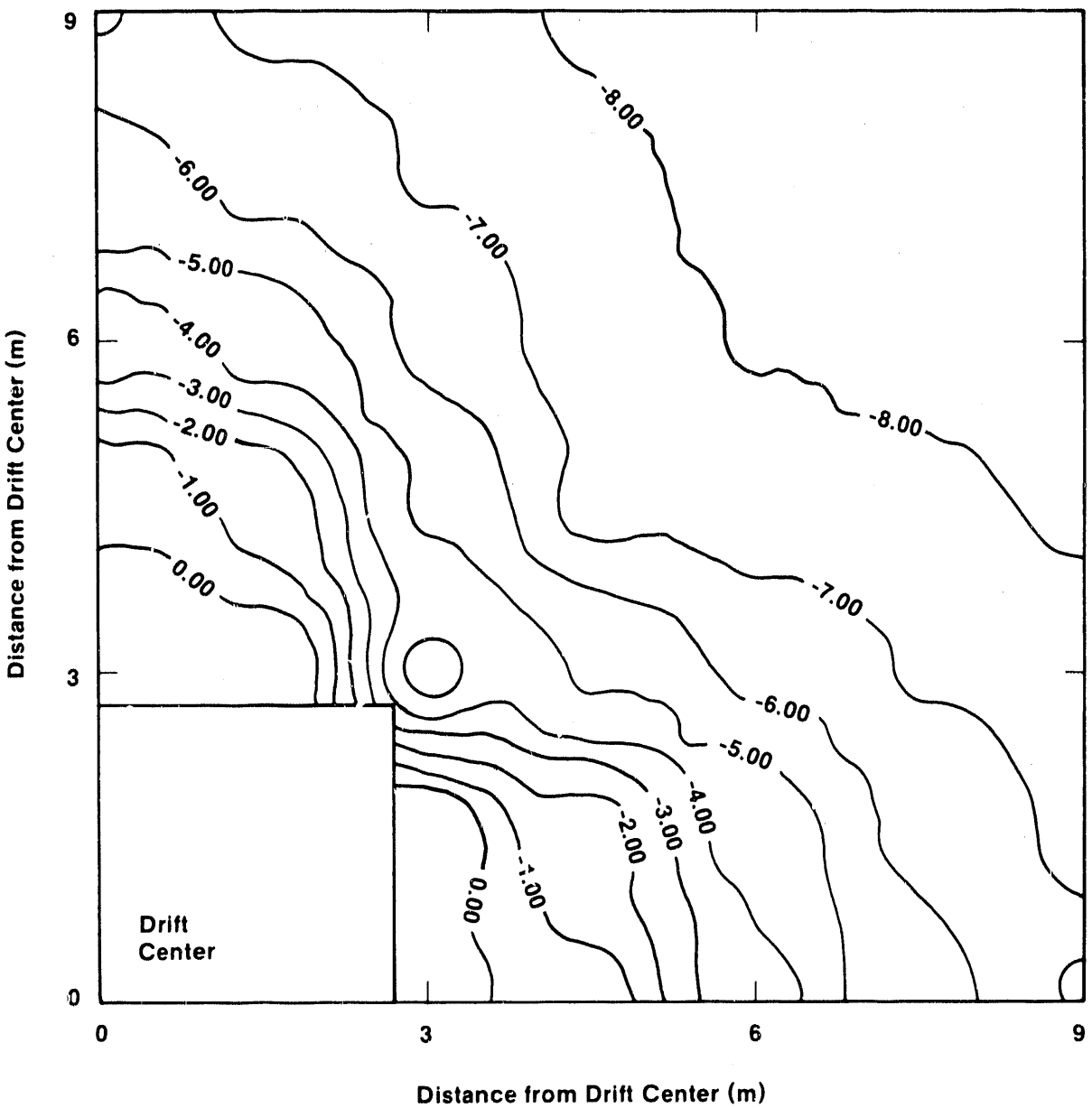

Figure 12. Contours of the failure criterion F surrounding a 5.4 m by 5.4 m drift immediately after excavation.

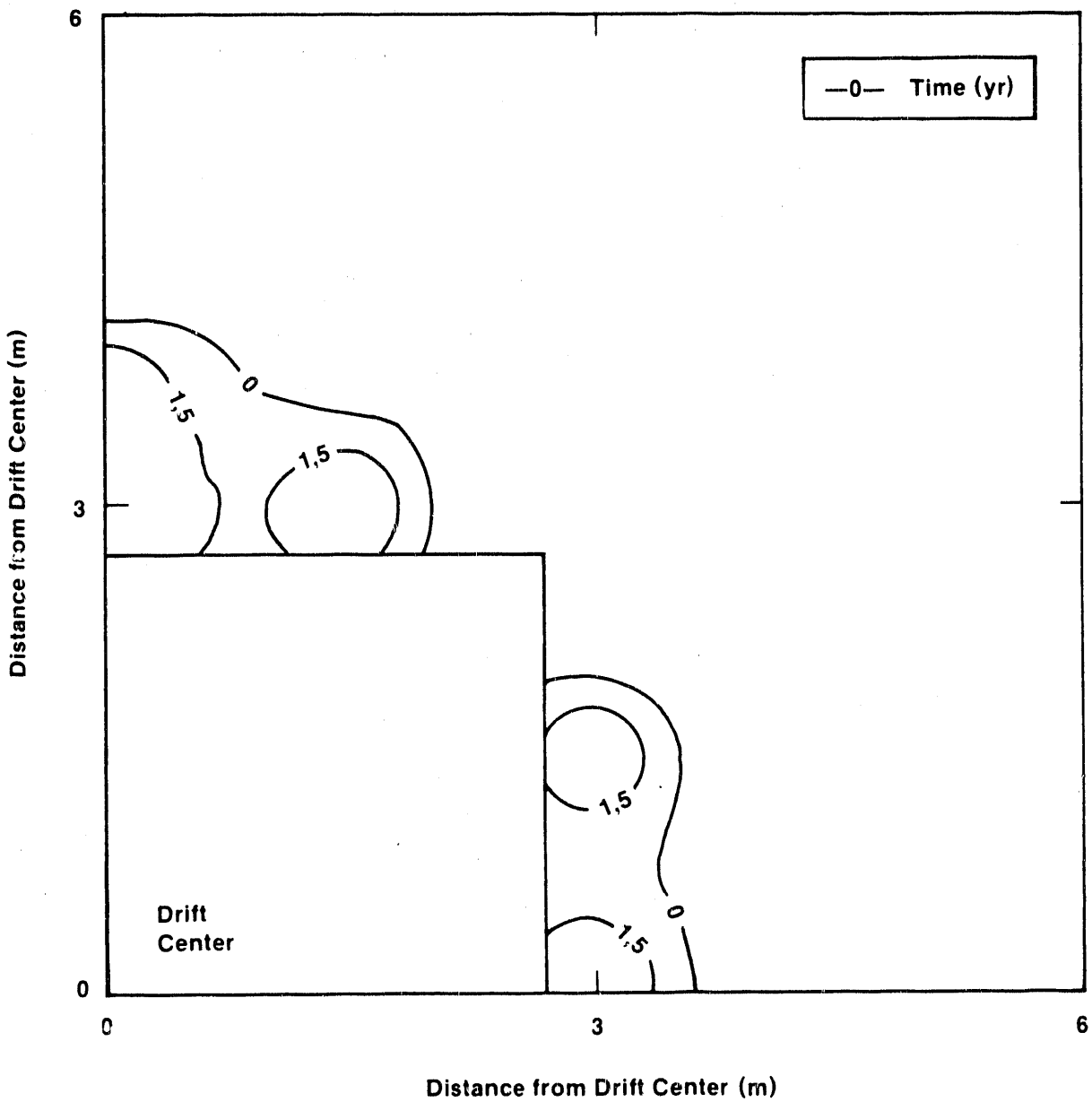

Figure 13. The F=0 contours at 0, 1 and 5 years after excavation surrounding a 5.4 m by 5.4 m drift.

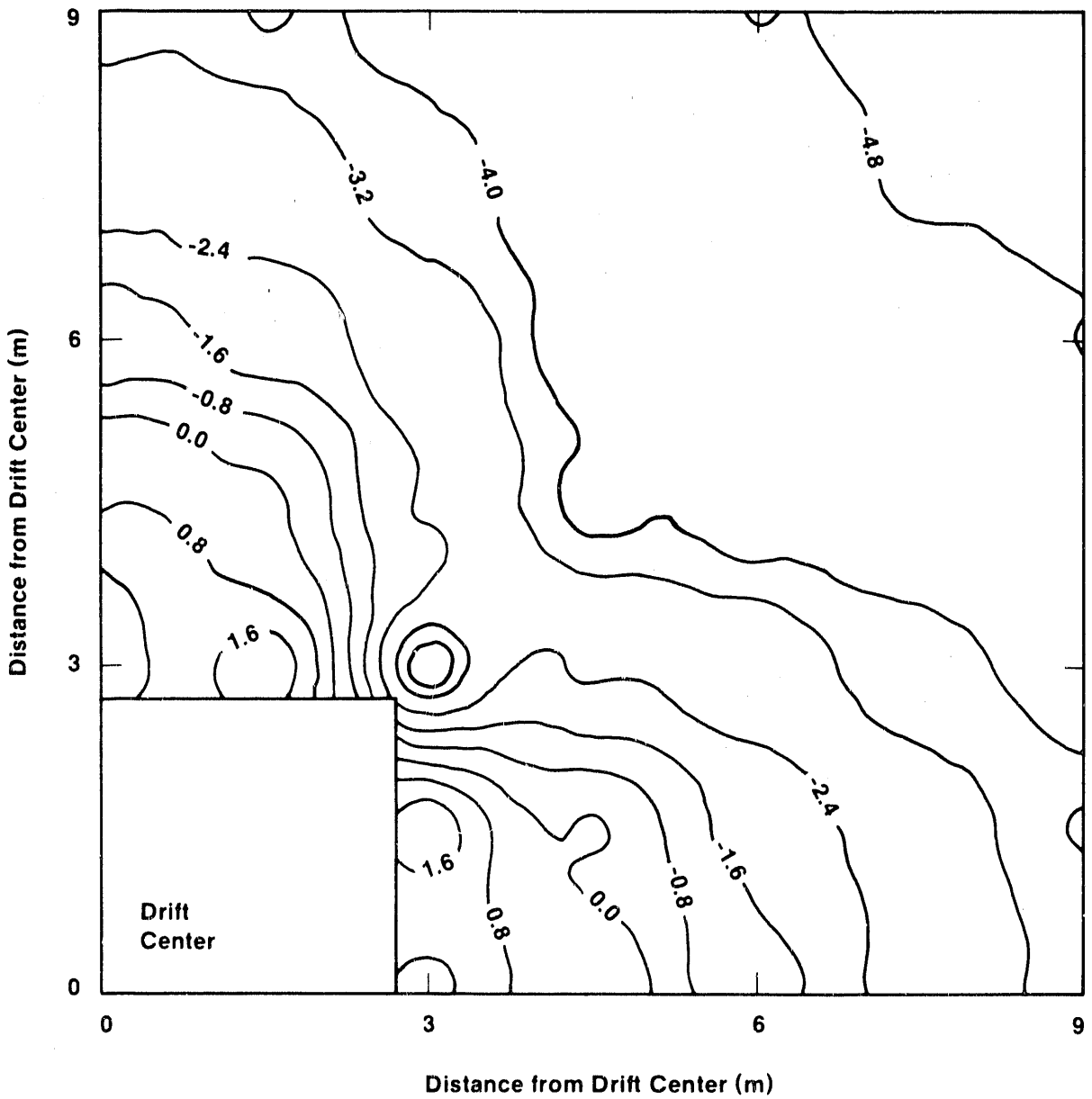

Figure 14. Contours of the crack initiation criterion M surrounding a 5.4 m by 5.4 m drift immediately after excavation.

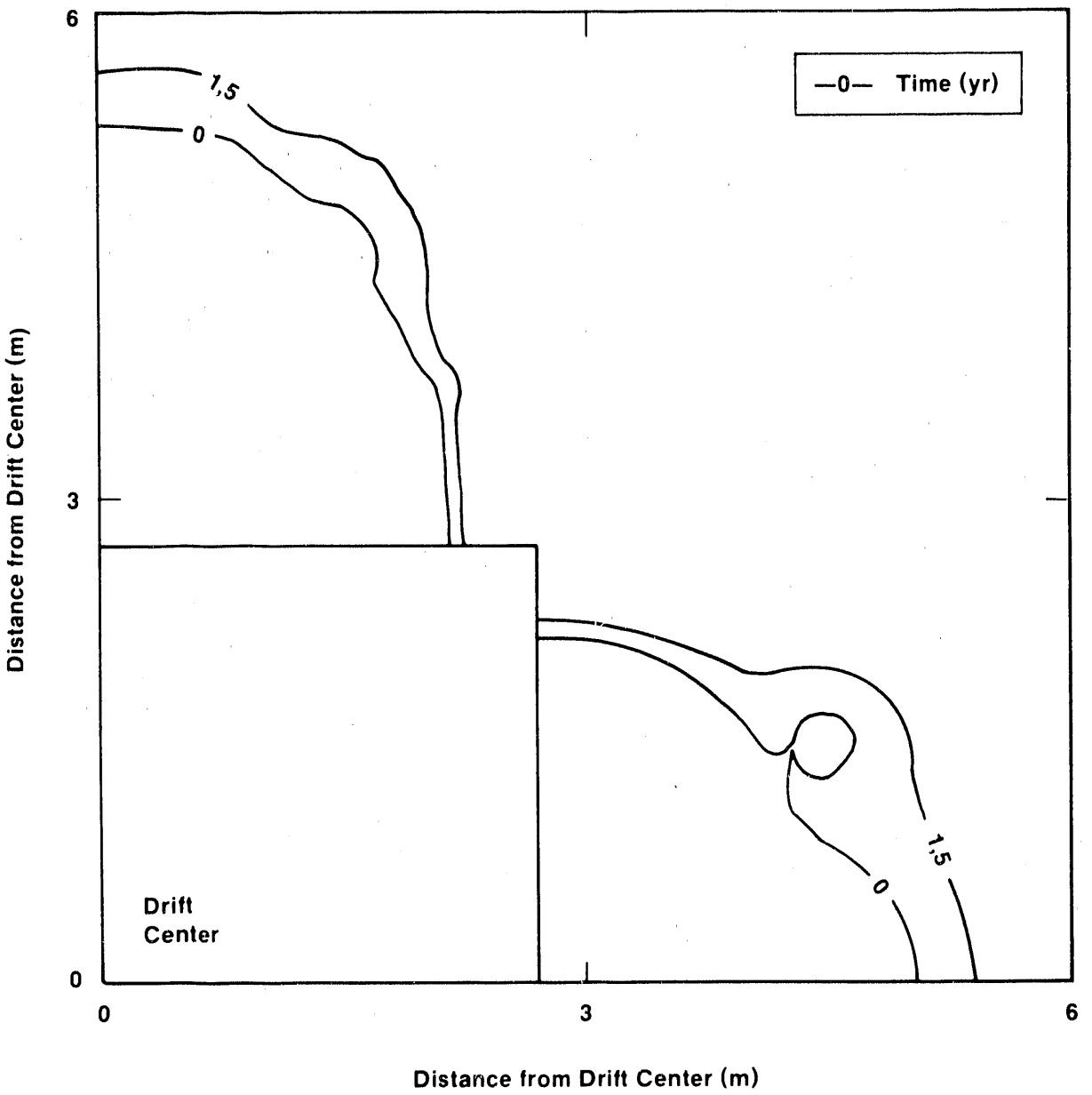

TRI-6346-11-0

Figure 15. The M=0 contours at 0, 1 and 5 years after excavation surrounding a 5.4 m by 5.4 m drift.

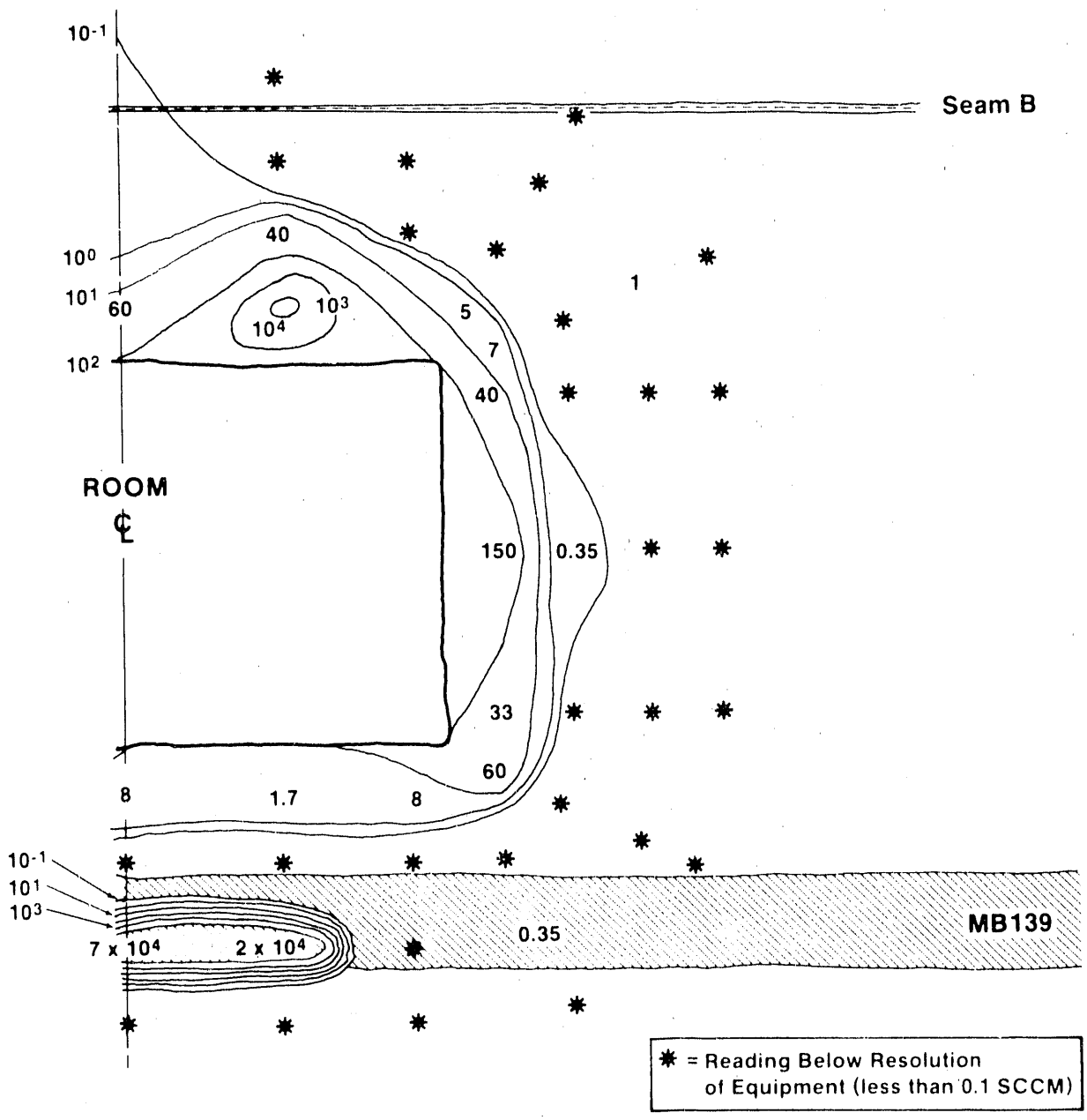

TRI-6330-82-3

Figure 16. Contours of gas flow rates surrounding a 3.0 m high by 6.0 m wide drift (after Borns and Stormont, 1988).

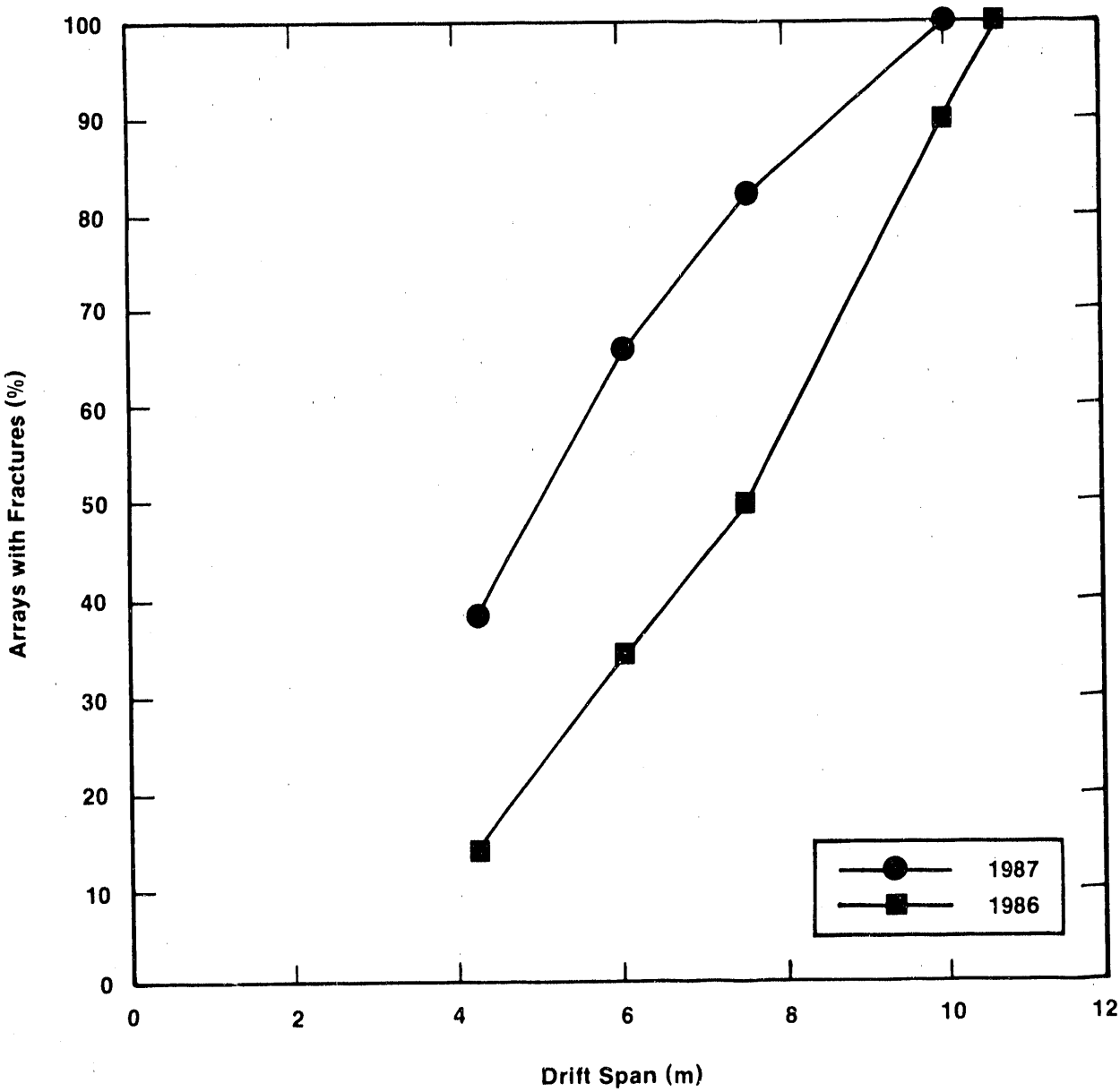

Figure 17. Results of fracture observations surveys in 1986 and 1987 (from USDOE, 1988).

END

DATE FILMED

01 / 17 / 91